JOURNAL OF CATALYSIS 138, 463–473 (1992)

Spectroscopic Characterization and Catalytic Properties of Sol-gel Pd/SiO_2 Catalysts

T. LOPEZ,* M. ASOMOZA,* P. BOSCH,* E. GARCIA-FIGUEROA,† AND R. GOMEZ*

*Department of Chemistry, Universidad Autonoma Metropolitana-Iztapalapa, A.P. 55-534, Mexico D.F. 09340; and †Instituto Mexicano del Petroleo, A.P. 14-805, Mexico D.F. 07730

Received March 24, 1992; revised June 22, 1992

The present study reports the results obtained by UV–VIS spectroscopy, FT–IR (Fourier transform infrared) spectroscopy, and BET area measurements of Pd/SiO_2 catalysts synthesized by the sol-gel process. This preparation technique results in the hydrolysis and polycondensation of a silicon alkoxide, which contains the metal halide salt $PdCl_2$ in the initial solution. The reaction takes place at pH 9, forming intermediates which correspond most probably to surface species $[SiO_2]-{}^{OH}_{[PdCl_2OHy]}$. The interaction between the silica gel and the palladium precursor has important effects on the specific surface area. The products are solids with BET specific areas up to 800 m^2/g. Catalytic tests (hydrogenation of 1-hexene and phenylacetylene) show that sol-gel catalysts exhibit high selectivity in the formation of 2-methylpentane and styrene. To explain the high selectivities shown by the Pd sol-gel catalysts a geometric effect induced by the support is proposed on the structure of the ca. 1-nm-size Pd metal particles.

INTRODUCTION

The factors affecting the dispersion of the active phase for supported transition metals have attracted the attention of various research groups. For the supported palladium catalysts employed in the ethylene oxidation reaction (*1*), it was found that the selectivity and conversion toward acetic acid depend on the surface palladium state. The reducing pretreatment of Pd(II) salts deposited on activated carbon directs the selectivity toward large quantities of acetaldehyde (*2, 3*). Detailed structural investigation on conventionally prepared Pd catalysts has revealed the structurally complex nature of the support and the difficulty of achieving very homogeneous states of dispersion (*4, 5*), i.e., the obtainment of very narrow particle distributions with diameters <20 Å is the major problem in the preparation of highly dispersed palladium catalysts.

With this purpose, Carturan *et al.* (*6*) using the method proposed by Yermakov (*7*), i.e., to anchor the precursor to the support, succeeded in preparing palladium supported on vitreous material. The dispersion obtained was high (*8, 9*). They propose that in liquid-phase reactions, such high dispersion can be correlated to the selectivity and the kinetics of the phenylacetylene hydrogenation. The anchoring method for obtaining a high metallic dispersion has been successfully achieved with various metals Ni, Pd, and Pt (*7, 10, 11*). The metal precursor used in these studies is an organometallic compound and the reactant is the –OH surface groups. Few examples have been reported using inorganic metallic salts (*4, 5*). It seems that the anchoring of the palladium salts on the support must occur through very reactive –OH surface groups.

The synthesis of silica by the sol-gel method, i.e., hydrolysis of $Si(OEt)_4$ forming highly reactive $\equiv$Si–OH species seems to be a good alternative for the preparation of highly dispersed metals. The $PdCl_2$ is added during the gelation step producing a strong interaction between the precursor and the –OH surface groups.

The catalysts obtained by this method show improved properties as recently re-

0021-9517/92 $5.00

ported for Ru/SiO_2 (*12, 13*) and Pt/SiO_2 (*14*) catalysts. The preparation process affects mainly the deactivation process in benzene hydrogenation and *n*-pentane hydrogenolysis. These results have lead us to try to find a relationship between the chemical environment produced during the impregnation step and the catalytic activity in sol-gel-prepared catalysts. With this purpose in mind in the present work, UV–VIS and FT–IR spectroscopies were used to study the interaction between the SiO_2 gel and the $PdCl_2$. Gas-phase hydrogenation of 1-hexene and phenylacetylene was chosen as the catalytic test for the reduced solids.

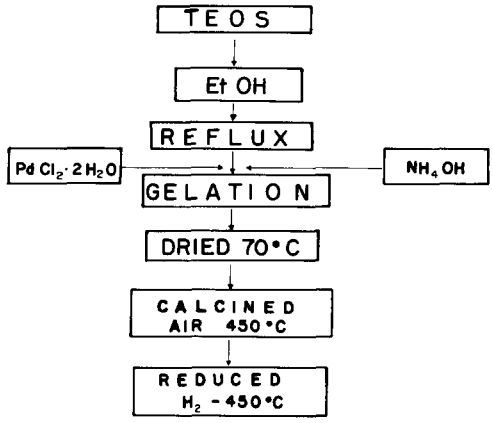

FIG. 1. Flow diagram for the sol-gel catalysts preparation.

EXPERIMENTAL

CATALYST PREPARATION

Sol-gel Catalysts

Pd-0.1. Tetraethoxysilane (TEOS) (24.1 ml, Aldrich 99.1%) reacts with 10 ml of ethanol (Baker, 99.99%) under reflux at 80°C and constant stirring. A solution containing 0.016 g of $PdCl_2 \cdot 2H_2O$ (ICN, 99.9%), 1.5 ml of NH_4OH (Baker, 35% vol NH_3), and 10 ml of distilled water is prepared and added to the refluxing mixture under stirring until the gel is formed. The metal concentration in the gel was 0.1% wt.

Catalysts Pd-0.3, Pd-0.5, and Pd-3.0. These materials were prepared in the same way as the former, but the quantity of $PdCl_2$ increases in such a way that the final metal concentrations were 0.3, 0.5, and 3.0% wt. The flow diagram summarizing the sol-gel preparations is shown in Fig. 1.

Impregnated Catalyst

Catalyst Pd–I-0.5. Three grams of silica Akzo F-2 (440 m^2/g) was impregnated with aqueous solution of $PdCl_2 \cdot 2H_2O$ (ICN, 99.9%) and 20 ml of distilled water; after 2 h of stirring, the excess water was evaporated under vacuum.

All the samples were divided into two portions: one that was dried at 70°C for 12 h (fresh samples) and another that was calcined at 450°C for 4 h (calcined samples).

DISPERSION MEASUREMENTS

Adsorption curves were measured by gravimetry using a Cahn RG-UHV electrobalance. Catalysts were reduced *in situ* at 450°C under flowing hydrogen (1.8 liter/h) for 4 h and then evacuated at 10^{-5} Torr for 4 h at the reduction temperature. Hydrogen and oxygen (Matheson UHP) were adsorbed at 70°C to inhibit hydride formation. Conditions and calculations were similar to those reported previously for Pt/SiO_2 catalysts (*14*).

UV–VIS AND FT–IR SPECTROSCOPIC CHARACTERIZATION

Calcined samples were characterized by UV–VIS (diffuse reflectance) in a CARY 17 D Varian spectrograph with an integrating sphere. The reference (MgO) was a 100% reflectance sample. IR spectroscopy was studied in dried samples at 70°C in a Nicolet MX-1 Fourier transform apparatus (FTIR), using transparent pellets of catalysts. This equipment graphs the wavenumber (x axis) in logarithmic scale.

SPECIFIC SURFACE AREA

In samples calcined at 450°C for 4 h and reduced at 450°C in flowing hydrogen, the surface area was determined in a Micromeritics Model 2300 using N_2 as adsorbent. To

obtain additional information about the texture, isotherms were made. The areas were calculated using the BET method.

X-Ray Diffraction Characterization

The X-ray diffraction patterns were obtained with a D500 Siemens diffractometer. The X-ray tube anode was copper and a diffracted beam monochromator selected the $K\bar{\alpha}$ radiation. To measure the cell parameters a corundum (α-Al_2O_3) standard was used. The mean crystallite size was estimated using the Debye–Scherrer equation (*15*).

In the case of small angle X-ray scattering (SAXS) studies, a Kratky camera and a Mo anode tube were used to measure the scattering curves. The collimation was such that an infinitely high beam could be assumed (*16*). As the metal-supported catalysts are a typical three-phase system (the support, the pores, and the metal particles), two approaches were compared. On one hand the three-phase system was solved mathematically as shown by Espinat *et al.* (*17*). On the other, the catalysts were impregnated with CH_3I (pore masking method) and the curves were studied as if the system consisted of two phases (*18, 19*). The distribution curves reported in this work are surface distributions, and they can be compared to the gas adsorption and electron microscopy results (*20*).

Determination of the Catalytic Activity

Catalytic activities were determined in most cases at low conversion (less than 5%). All the samples were reduced in flowing hydrogen for 4 h at 450°C before activity measurements. The rates were measured in a conventional flow reactor. The conditions for 1-hexene (Aldrich 99.9%) hydrogenation were reaction temperature, 30°C; hydrocarbon partial pressure, 40 Torr; and H_2 partial pressure, 720 Torr. Activities for phenylacetylene (Aldrich 99.9%) were determined at reaction temperature, 30°C; hydrocarbon partial pressure, 5 Torr; and hydrogen partial pressure, 755 Torr. Under these conditions the only detected products were 2-methylpentane and *n*-hexane for the former reaction and styrene and ethylbenzene for the phenylacetylene hydrogenation.

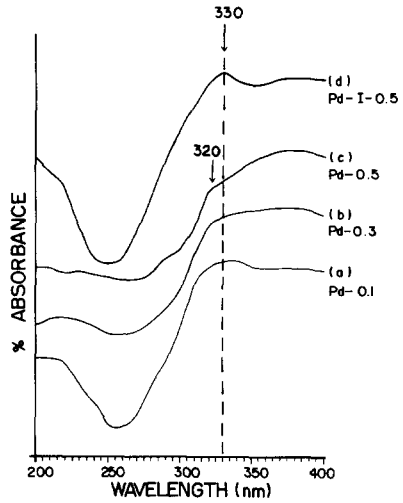

FIG. 2. UV (200–400 nm) diffuse reflectance spectra of Pd/SiO_2 catalysts.

RESULTS AND DISCUSSION

UV–VIS and FT–IR Spectroscopic Study

The UV–VIS (diffuse reflectance) bands found in the catalysts calcined at 450°C are shown in Fig. 2. The metal in the sol-gel samples forms a square planar complex with a D_4h symmetry. These compounds are diamagnetic d^8 low spin whose ground state configuration is $[t_{2g}\ (xz, yz, xy)]^8$.

The band at circa 220 nm is assigned to a charge transfer transition (CT) transition between σ_{Cl} orbitals and the empty metal orbital $(x^2 - y^2)$: $e_u L_\sigma \rightarrow b;_{1g}\ \sigma^*$; $[^1A_{1g} \rightarrow {}^1E_u]$, spin-allowed transition (*21*).

In Fig. 2, a shift of the CT band by metal content can be observed. The shift of the bands to higher energy for low metal content catalysts can be atributed to an exchange between the Cl^- ions and the hydroxyl groups of the silica support in the metal coordination sphere. The ligand σ orbital and the empty metal orbital $(x^2 - y^2)$ are closer in the Pd-0.1 and Pd-0.3 catalysts. At low

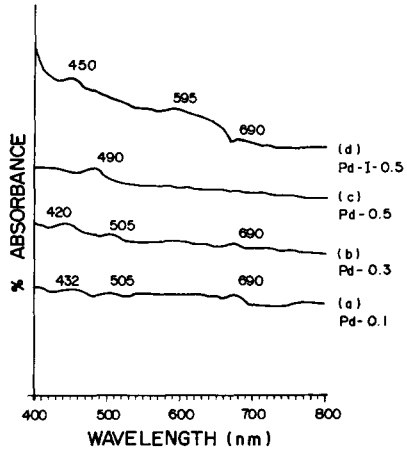

FIG. 3. Visible (400–800 nm) diffuse reflectance spectra of Pd/SiO_2 catalysts.

metal content the interaction between the highly hydroxylated silica and the precursor $PdCl_2$ will be the highest. The CT band is not observed in the Pd–I-0.5 catalyst with silica F-2 as support, since in this support the silica surface is practically dehydroxylated and the chlorine exchange does not occur: the $PdCl_2$ remains as a planar compound.

The bands observed around 330, 420, 500, and 690 nm (Figs. 2 and 3), are *d-d* transitions (*22*):

$$^1A_{1g} \text{——} ^1B_{1g};\quad \sigma_{Cl} \text{——} (x^2 - y^2)Pd$$
$$^1A_{1g} \text{——} ^1E_g;\quad \pi_{Cl} \text{——} (x^2 - y^2)Pd$$
$$^1A_{1g} \text{——} ^1B_{1g};\quad \pi_{OH} \text{——} (x^2 - y^2)Pd.$$

The position of these bands was interpreted by Michel *et al.* (*23*) in the study of silica impregnation with $PdCl_2$. They attributed these bands to the formation of a tetrachloropalladate complex in HCl solution. The position of these bands is in agreement with our results (Fig. 3). However, they are shifted to high energy in sol-gel catalysts. This shift could be a consequence of the distortion of the square planar complex due to the strong interaction with the hydroxyls of the silica support. To support this interpretation, it could be interesting to pay attention to the band observed at around 330 nm. It has been assigned by Rasmussen and Jorgensen (*24*) to the complex containing chlorine in Pd/SiO_2 catalyst, while the band observed at around 500 nm has been attributed to the presence of hydroxyl groups in the complex.

The bands obse ved in the impregnated Pd–I-0.5 catalyst ai e also reported in Figs. 2 and 3. Note the 330-nm chlorine band of this catalyst. However, the band assigned to the hydroxyl interaction is largely shifted to 595 nm. This shift is probably due to the formation of the solvated complex containing H_2O in the coordination sphere (*25*).

The formation of the square planar complex into the reactant solution is produced by a strong interaction quite different to the one observed in conventional impregnation and must occur during the condensation step of the SiO_2 formation as described in Fig. 4.

Vibration spectroscopy is a powerful technique for studying the structure of the glass and it has been used in the last few years. Although it does not usually provide direct structural information, it can be a

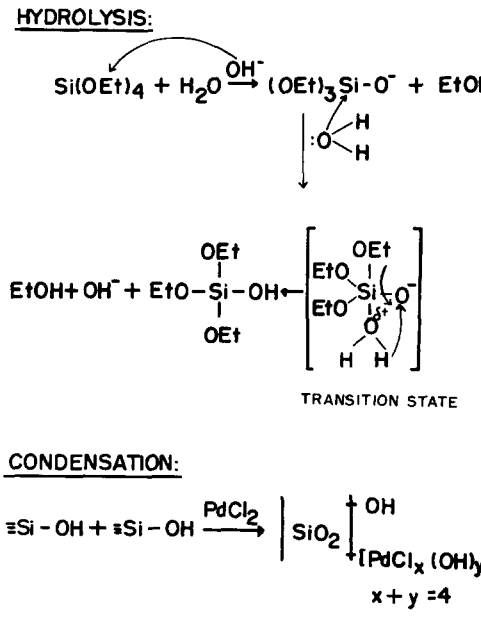

FIG. 4. Scheme of the gelation reaction mechanism.

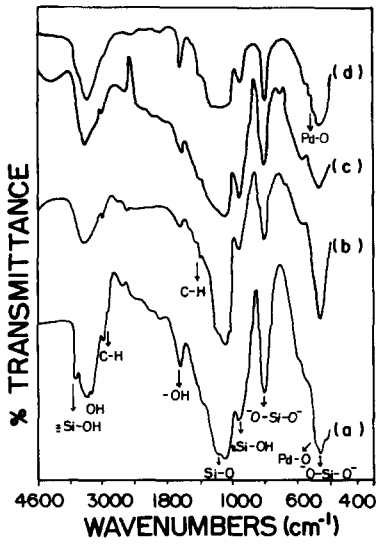

FIG. 5. FT–IR spectra of Pd/SiO_2 samples: (a) Pd-0.1, (b) Pd-0.3, (c) Pd-0.5, and (d) Pd–I-0.5.

very useful tool for probing terminal or weakly coupled Si–O–Si bridging atoms in terms of short-range order (*26–28*).

The IR spectra of the samples dried at 70°C show (Fig. 5) that the band due to the OH groups of silanols, water, and ethanol is located within the region of 3500 to 3400 cm^{-1} for the sol-gel materials and at 3300 cm^{-1} for the impregnated one; this shift to a lower-energy region shows that in Pd–I-0.5, the interaction between the metal and silica OH is weak. At 1630 cm^{-1} the OH flexion vibration due to the occluded water of the gels appears (*29, 30*).

The high-frequency IR-active mode peak near 1070 cm^{-1} accompanied by a small shoulder was assigned to antisymmetric stretching of the bridging oxygens along a line parallel to Si–Si with a substantial silicon motion. This band shifts toward a lower energy because of the metal concentration. At 950 cm^{-1} the silanol stretching vibration appears in the Pd–I-0.5 sample; this band shifts to 966 cm^{-1} in the sol-gel preparations due to a stronger metal–support interaction (*26*).

At 800 and 470 cm^{-1} two bands respectively, are observed corresponding to a completely symmetric vibration of the nucleophiles. It involves a symmetric stretching motion of all the bridging oxygens around the bisectors of the Si–O–Si intertetrahedral angles θ about fixed silicon atoms. Finally the stretching band Pd–O (*31*) in Pd–I-0.5 sample is observed at 690 cm^{-1}; that band is found at lower energy regions in the sol-gel samples at 536 cm^{-1} (*32*).

Specific Surface Area Study

Palladium added to the homogeneous initial solution induces a process of nucleation during the gelation reaction. The structure of the compounds evolves with hydrolysis and condensation reactions, passing from a colloidal solution to a solid with a well-defined microcrystalline structure. The interaction of palladium with the silica gel has an important effect on the specific area of solids calcined at 450°C for 4 h and reduced also at 450°C for 4 h (Table 1). This process should ensure a high metal dispersion. In the impregnated sample the area is 372 m^2/g, whereas in the sol-gel materials it is more than 600 m^2/g. Note that the silica support prepared without palladium shows a BET area of only 110 m^2/g.

Representative isotherm and pore size distribution of the palladium sol-gel catalysts are shown in Figs. 6 and 7, respectively. It can be seen that the Pd-0.5 sol-gel catalyst has small pores and a very narrow pore size distribution, as determined by adsorption–desorption isotherm.

Metallic Dispersion

The particle size for the various catalysts obtained by chemisorption is reported in Table 2. To compare these results, particle size

TABLE 1

Specific Surface BET Areas of the Pd/SiO_2 Sol-gel Catalysts

Catalysts:	Pd-0.1	Pd-0.3	Pd-0.5	Pd-3.0	Pd-I-0.5.
Area (m^2/g):	889	817	634	630	372

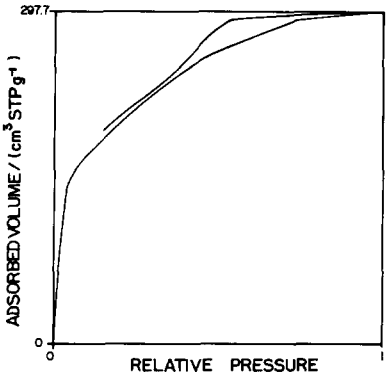

FIG. 6. Nitrogen adsorption isotherm for Pd-0.5 catalyst.

distributions obtained from electron micrographs (JEOL 100×) are shown in Fig. 8. An average surface size diameter ($\Sigma n_i d_i^3 / \Sigma n_i d_i^2$) can be computed and the values are reported in Table 2.

The results show a very narrow particle size distribution; most particles are smaller than 10 Å. The comparison between chemisorption and electron microscopy shows that in all the cases both methods agree. Nevertheless some electron micrographs for sol-gel-reduced Pd-0.5 and Pd-3.0, shown in Figs. 9 and 10, presented larger particles.

X-Ray Study

No PdO_2 or PdO X-ray diffraction lines were detected; only the Pd(111) peak was

TABLE 2

Comparative Particle Size (Å) in Sol-gel Catalysts, Determined by Chemisorption (Φ_q) and Electron Microscopy (Φ_{me})

Catalysts	Pd-0.1	Pd-0.3	Pd-0.5	Pd-3.0	Pd–I-0.5
Φ_q	10	11	10	25	22
Φ_{me}	<10	<10	15	22	24

present in both reduced catalysts (0.5% wt Pd and 3% wt Pd sol-gel). From these (111) interplanar distances, corrected with the error determined with the α-Al_2O_3 lines, the cell parameters were estimated and compared to the value reported in the 5-0681 JCPDS card. The very small differences fall into the experimental error range. These crystallites are then Pd. The crystallite sizes (84 Å) do not agree with the gas adsorption and the electron microscopy results previously reported. It must be remembered, indeed, that very small crystallites (less than 40 Å) are not measured with conventional X-ray diffraction technique. The suitable method is, in such a case, the SAXS.

The SAXS curve of the desorbed catalysts was studied as shown by Espinat *et al.* (*17*) for three-phase materials. The distribution curves are compared in Fig. 11. Only one well-defined peak is observed for each catalyst; the maxima are found at $D = 22$ Å (0.5% Pd/SiO_2) and $D = 26$ Å (3.0% Pd/

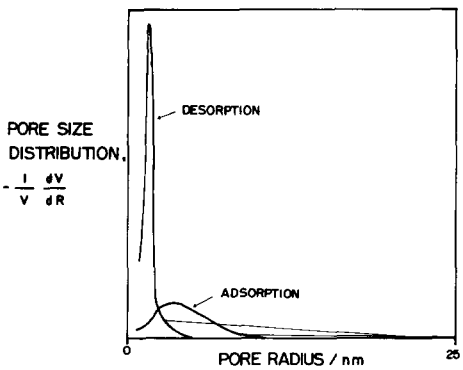

FIG. 7. Pore size distribution for Pd-0.5 catalyst.

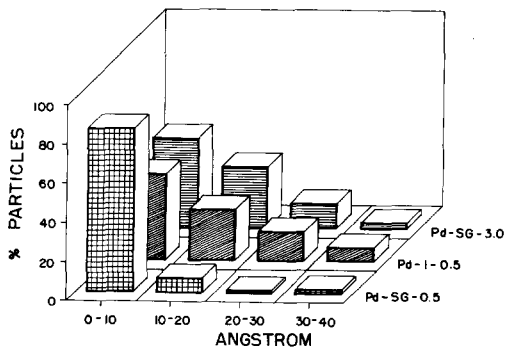

FIG. 8. Pd particle size distribution vs diameter for sol-gel and impregnated palladium catalysts.

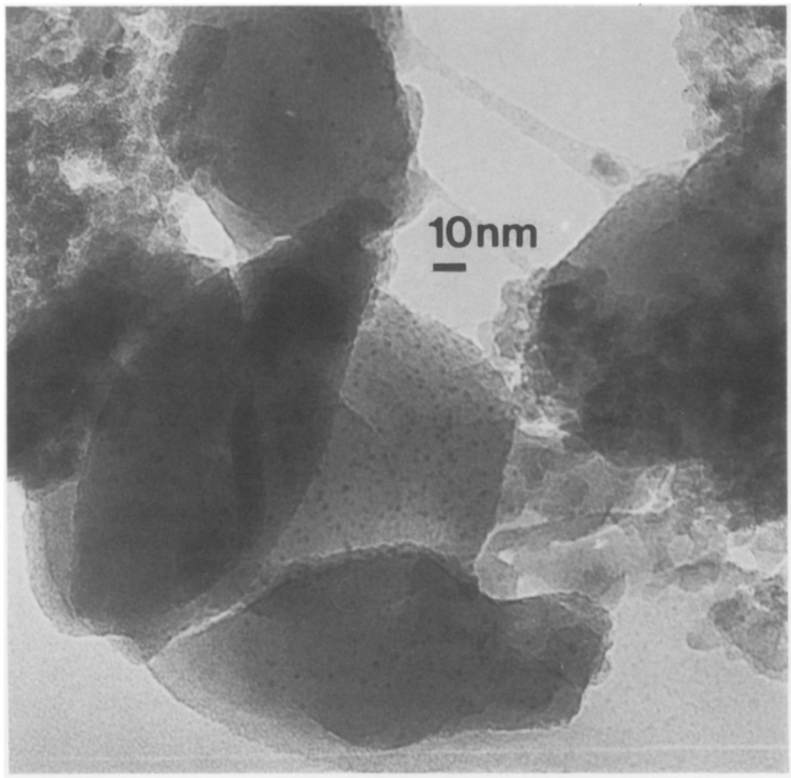

FIG. 9. Electron micrograph of Pd-0.5 sol-gel catalyst.

SiO_2). The catalysts are then monodisperse and this result is in good agreement with the measured particle sizes by TEM and chemisorption, although some very large crystallites are present in both catalysts as shown by X-ray diffraction.

For comparison purposes the CH_3I-impregnated catalysts were studied by SAXS in the usual way (two phases). The metal particle size distributions are shown in Fig. 12. In both catalysts the distributions are very broad and the two peaks are found around D=30–38 Å and D=62–68 Å. These results are not in agreement with those obtained with the other techniques. This difference must be attributed to ineffective pore masking by CH_3I. If the water desorption of the sample is not total and the CH_3I penetration is not good enough the pores are "half masked," i.e., a microporosity is created because of the partial filling of the pores. Another possibility could be that a fraction of the pores is not accessible to the CH_3I. It seems then that the pore masking technique is not the most adequate for obtaining the metal particle size distribution in sol-gel microporous catalysts. The mathematical resolution of the three phase problem seems much more effective.

Catalytic Activity Study

The results obtained in 1-hexene hydrogenation are reported in Table 3. Activities per site can be considered essentially constant for all the catalysts; variations in specific rate of 80% are difficult to interpret in terms of intrinsic metallic properties. These results show that the activity in palladium atoms can be considered independent of the preparation method (sol-gel or impregnation). However, the selectivity to isomerized 2-pentane is quite different in sol-

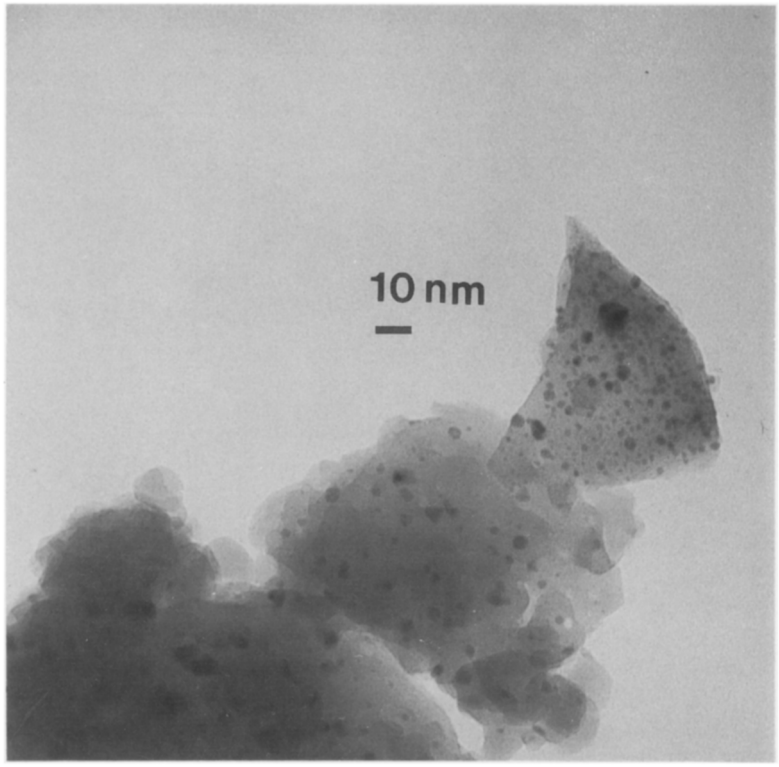

FIG. 10. Electron micrograph of Pd-3.0 sol-gel catalyst.

gel catalysts from that observed in impregnated catalysts. Selectivity (defined as the ratio 2-isopentane/2-isopentane + *n*-hexane products) is higher in sol-gel preparations.

A similar behavior is observed in the study of the hydrogenation of phenylacetylene; i.e., selectivity is very different in sol-gel catalysts. Styrene is the principal product in sol-gel catalysts while in impregnated ones ethylbenzene is the major product (Table 4).

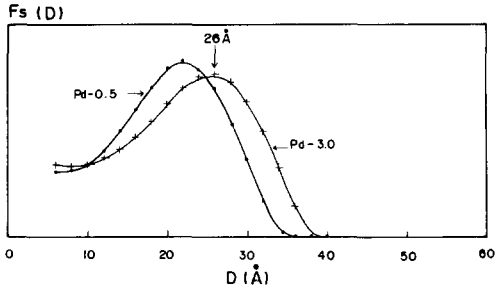

FIG. 11. SAXS surface metal particle distribution vs diameter of the 3.0 and 0.5% sol-gel Pd catalysts, three-phase method. The curves are not normalized.

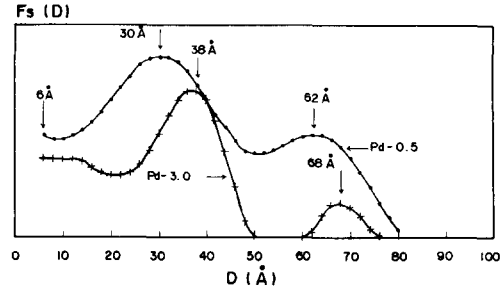

FIG. 12. SAXS surface metal particle size distribution vs diameter of the 3.0 and 0.5% sol-gel Pd catalysts, pore masking method. The curves are not normalized.

TABLE 3

Catalytic Activity and Selectivity to 2-Methylpentane (2MP) and *n*-Hexane (nC_6) in Pd/SiO_2 Sol-gel Catalysts: Hydrogenation of 1-Hexene at 30°C

Catalysts	Specific rate 10^5 (mol/s mg Pd)	Activity by site 10^2/(molecules/site/s)	Selectivity %	
			2MP	nC_6
Pd-0.1	5.7	31	22	78
Pd-0.3	1.8	36	18	82
Pd-0.5	2.5	40	19	81
Pd-1.0	2.4	43	21	79
Pd-2.0	2.6	46	22	78
Pd-3.0	3.0	78	22	78
Pd–I-0.5	2.9	76	0	100

The behavior observed in sol-gel catalysts can be explained by two hypotheses: (i) modification of the electronic state of the palladium (*33*) by oxidizing centers of the support formation of Pd^+ species (electronic effect) and (ii) formation of small clusters (*34*), with remarkably different properties from those formed in impregnated catalysts (geometric effect). The first hypothesis requires supports with strong acid or basic properties and silica usually does not present this characteristic. However, if silica is heated in H_2 at 450°C in the presence of a transition metal (Pd), it may be activated by hydrogen spillover. Strong acidic properties may be developed (*35*, *36*). Furthermore, the silica in sol-gel catalysts presents a very high surface area and may be reactive to the spilled-over hydrogen. The conventional F-2 is less (or not) activated by hydrogen because it is less divided. Hence such an acidic support may be active in the reaction and may also alter the palladium electronic state.

The second hypothesis also seems to be probable. The formation of very small (<15 Å) palladium particles may imply the presence of electron-deficient species. Nevertheless electron microscopy characterization of the sol-gel Pd-3.0 and the impregnated catalyst Pd–I-0.5 shows that in both catalysts the particle size is of the same order, so particle size effects can be ruled out in these catalysts.

Selectivity to olefin formation in acetylenic compounds hydrogenated over palla-

TABLE 4

Catalytic Activity and Selectivity to Styrene and Ethylbenzene (EBZ) over Pd/SiO_2 Sol-gel Catalysts: Hydrogenation of Phenylacetylene at 30°C

Catalysts	Specific Activity 10^6 (mol/s mg Pd)	Activity by site 10^2/(molecules/site/s)	Selectivity %	
			Styrene	EBZ
Pd-0.1	10.9	81	95	5
Pd-0.3	5.1	72	95	5
Pd-0.5	2.3	58	97	3
Pd-1.0	3.8	53	99	1
Pd-2.0	3.2	61	93	7
Pd-0.3	1.2	96	96	4
Pd–I-0.5	3.5	78	15	85

dium catalysts is related to the dissolution of H_2 in large particles (*37*). Small particles are more effective for the formation of double bonds. The small particle size observed in both catalysts makes it difficult to assume that the differences in selectivity are related to differences in hydrogen dissolution. The phenomenon observed, then, in sol-gel catalysts, may be an effect of support acidity. Last but not least, another possible cause could be the shape of the metallic palladium particles formed during the preparation. The number of corner atoms, for instance, whose coordination is different from the coordination of face atoms depends on the shape of the particle. Also, the morphology of the particle determines the planes presented to the reactants. The small clusters arising from a strong interaction between the $PdCl_2$ precursor and the ≡SiOH groups, occurring during the preparation step, may influence the shape of the metallic particles. A particular form of the palladium clusters may be stabilized by the sol-gel support. If the Pd/SiO_2 sol-gel-prepared catalysts are similar to supported Rh catalysts (*34*), this interpretation can be used to explain the selectivity effect observed in palladium sol-gel catalysts.

CONCLUSIONS

The foregoing results show that the preparation of palladium-supported catalysts by the sol-gel method leads to the formation of $[SiO_2]_{-[PdCl_xOHy]}^{-OH}$ species with an unusual interaction detected by UV–VIS and FT–IR spectroscopies. The sol-gel method leads to unusual properties of supported Pd catalysts: (i) specific surface areas higher than 800 m^2/g, (ii) formation of small Pd particles <10 Å, (iii) catalysts exhibiting high selectivity to the formation of 2-methylpentane in the hydrogenation of 1-hexene, as well as very high selectivity to the formation of styrene in the hydrogenation of the phenylacetylene. As one of the Reviewers noted, the effect of chlorine cannot be neglected. However, all the catalysts (impregnated or sol-gel) were prepared from the same $PdCl_2$ precursor, so the chlorine content must be the same in each. The effect of chlorine will be presented in a subsequent work.

ACKNOWLEDGMENTS

This work was supported by Conacyt-OEA, SEP-Mexico grants. We thank the Instituto Mexicano del Petroleo for the use of SAXS facilities and V. H. Lara for the technical help.

REFERENCES

1. Kemball, C., and Patterson, W. R., *R. Soc. London A* **270,** 219 (1962).
2. Gerberich, H. R., Cant, N. W., and Hall, W. K., *J. Catal.* **16,** 204 (1970).
3. Cant, N. W., and Hall, W. K., *J. Catal.* **16,** 220 (1970).
4. Pope, D., Smith, W. L., Eastlake, M. G., and Moss, A. R., *J. Catal.* **22,** 72 (1971).
5. Benedetti, A., Cocco, G., Enzo, S., Piccaluga, G., and Schiffini, L., *J. Chim. Phys.* **78,** 961 (1981).
6. Carturan, G., Facchin, G., Cocco, G., Enzo, S., and Navazio, G., *J. Catal.* **76,** 405 (1982).
7. Yermakov, Yu. I., *Catal. Rev.* **13,** 77 (1976).
8. Cocco, G., Schiffini, L., Strukul G., and Carturan, G., *J. Catal.* **65,** 348 (1980).
9. Carturan, G., Cocco, G., Schiffini L., and Strukul, G., *J. Catal.* **65,** 359 (1980).
10. Yermakov, Yu. I., and Kuznetzov, B. N., *Kinet. Catal.*, **18,** 1167 (1977).
11. Yermakov, Yu. I., and Kuznetzov, B. N., *J. Mol. Catal.* **9,** 13 (1980).
12. Lopez, T., Lopez Gaona A., and Gomez, R., *J. Non-Cryst. Solids* **110,** 170 (1989).
13. Lopez, T., Lopez Gaona A., and Gomez, R., *Langmuir* **6,** 1343 (1990).
14. Lopez, T., Romero A., and Gomez, R., *J. Non-Cryst. Solids* **127,** 105 (1991).
15. Klug, H., and Alexander, R., "X-ray Diffraction Procedures." Wiley, New York, 1994.
16. Sole, J. L., *J. Phys. Radium* **18,** 90 (1957).
17. Espinat, D., Moraweck, B., Larua, J. F., and Renouprez, A. J., *Appl. Cryst.* **17,** 411 (1984).
18. Renouprez, A. J., Hoang Van, C., and Compagnon, P. A., *J. Catal.* **34,** 411 (1974).
19. Dartigues, J. L., Chambellan, A., Corolleur, S., Gault, F., Renouprez, A., Moraweck, B., Bosch, P., and Dalmai Imelik, B., *Nouv. J. Chim.* **3,** 691 (1979).
20. Dominguez, J. M., Bosch, P., and Yacaman, M., *Rev. Inst. Mex. Petroleo* **15,** 66 (1983).
21. Rush, RM, Martin D. S., and LeGrand, R. G., *Inorg. Chem.* **14,** 2543 (1975).
22. Basch, H., and Gray, H. B., *Inorg. Chem.* **6,** 365 (1967).
23. Michel, L., Hoang-Van, C., and Bozon-Verduraz, F., *New J. Chem.* **2,** 575 (1978).

24. Rasmussen L., and Jorgensen, C. J., *Acta Chem. Scand.* **22,** 365 (1968).
25. Bozon-Verduraz, F., Omar, A., Escard J., and Pontvianne, B., *J. Catal.* **53,** 126 (1978).
26. Almeida, R. M., *J. Non-Cryst. Solids* **106,** 347 (1988).
27. Yoshino, H., Kamiya K., and Nasu, H., *J. Non-Cryst. Solids* **126** (1990).
28. Stolen, R. H., and Walrafen, G. E., *J. Chem. Phys.* **64,** 2623 (1976).
29. Galeneer, F. L., *J. Non-Cryst. Solids* **49,** 53 (1982).
30. Burneau, A., Barres, O., Gallas, J. P., and Lavalley, J. C., *Langmuir* **6,** 1364 (1990).
31. Nakamoto, K., "Infrared Spectra of Inorganic and Coordination Compounds," 2nd ed. Wiley, New York, 1970.
32. Lippert, J. L., Melpolder S. B., and Kelts, L. M., *J. Non-Cryst. Solids* **104,** 139 (1988).
33. Carturan, G., Facchin, G., Gottardi, V., Guglielmi, M., and Navazio, G., *J. Non-Cryst. Solids* **48,** 219 (1982).
34. Yates, D. J. C., Murrel, L. L., and Prestidge, E. B., *J. Catal.* **57,** 41 (1979).
35. Teichner, S. J., *J. Catal.* **115,** 591 (1989).
36. Lacroix, M., Pajonk, G. M., and Teichner, S. J., *J. Catal.* **101,** 314 (1986).
37. Weels, P. B., *J. Catal.* **52,** 498 (1978).